ISSN 2181-8622

Manufacturing technology problems

Scientific and Technical Journal Namangan Institute of Engineering and Technology

INDEX COPERNICUS INTERNATIONAL

Volume 8
Issue 4
2023

Google Scholar
Crossref doi
SLIB.UZ Scientific library of Uzbekistan

6. Tilloev L.I., Usmanov H.R. The mechanism of formation of waste yellow oil // Materials of the scientific-practical international conference on the topic "Innovative ways of solving the current problems of the development of food, oil, gas and chemical industries". Bukhara: – 2019. Volume 2. pp. 216-219.

7. Patent US 5220104 A Method for the prevention of fouling in a caustic solution. Cato R. McDaniel, Paul V. Roling. Filed: Jun. 15, 1992. Appl. No.: 898,976

8. Tilloyev L.I., Dostov H.B. Formation, composition and properties of waste - yellow oil // "Innovative solutions of current problems in the field of metalorganic high molecular compounds" International scientific and practical online conference. Tashkent: - 2021. Volume 3. pp. 309-311.

9. Patent US 4673489 A Method for prevention of fouling ina basic solution by addition of specific nitrogen compounds. Paul V. Rolling. Fied: Oct. 10, 1985. Appl. No.: 786,274

10. Patent US 5160425 A Method of inhibiting formation of fouling materials during basic washing of hydrocarbons u.s. patent documents contaminated with oxygen compounds. Vincent E. Lewis. Filed: Jun. 21, 1991. Appl. No.: 718,623

Patent US 6372121 B1 Reducing undesired polymerization in the basic wash unit of hydrocarbon cracking process. Robert D. McClain, Natu R. Patel, Raymond M. Glath. Filed: Oct. 31, 2000. Appl. No.: 09/703,108

EFFECT OF TEMPERATURE ON PHOTOELECTRIC PARAMETERS OF THREE-WAY ILLUMINATED SOLAR CELLS

MIRZAALIMOV AVAZBEK

Senior Teacher of Andijan State University
E-mail.: avazbek.mirzaalimov@mail.ru, phone.: (+99897) 273 4808

Abstract:

Objective. Increasing the efficiency of solar cells and reducing the amount of material used in its production is one of the important tasks of today.

Methods. A 3-way sensitive solar cell was designed for this purpose. Compared with one surface, the efficiency of three surfaces increased by 2,81 times and two surfaces by 1,72 times. One of the main parameters of the environment is temperature. The daily temperature changes according to the seasons. Therefore, it is important to study the effect of temperature on solar elements.

Results. In this scientific work, the effect of temperature on the photoelectric parameters of a three-way sensitive silicon-based solar cell was studied. It was found that the temperature coefficients of the photoelectric parameters of the three-way sensitive solar cell do not change when different areas are illuminated.

Conclusion. It was determined that the temperature coefficient of the operating voltage is $2{,}52\times10^{-3}$ V/K, and the temperature coefficient of the filling factor is $1{,}8\times10^{-3}$ K^{-1}. In addition, when the temperature changed from 300K to 350K, the short-circuit current in the three-side light state decreased by 4%.

Keywords: Three-way sensitive, solar cell, silicon, modeling, sunlight.

Introduction. Along with the increase in the need for energy, the use of renewable energy sources is also increasing. Because renewable energy sources are the best solution to today's energy shortage without harming the environment [1]. According to the International Energy Agency, in 2021 the volume of renewable energy sources reached 276 GW. Among renewable energy sources, solar energy is widely used to obtain heat and electricity [2]. Solar cells are mainly used to convert solar energy into electricity. 85% of solar cells produced in industry are silicon-based solar cells [3]. Therefore, a silicon-

based solar cell was chosen as a research object in this scientific work. According to theoretical calculations, the maximum efficiency of a silicon-based solar cell does not exceed 29% [4]. Scientific work is being carried out to increase the efficiency of the silicon-based solar cell and reduce its cost. For example, in order to reduce the surface recombination and improve the optical properties of a silicon-based solar cell, its surface is covered with SiNx with a thickness of 75 nm or SiO_2 with a thickness of 100 nm [5]. In addition, it has been found that the incorporation of metal nanoparticles into a silicon-based solar cell increases the efficiency [6]. Dual-sensitive silicon-based solar cells have been designed to increase the amount of electricity produced [7]. In the experiment, the efficiency of the front side of the double-sensing silicon-based solar cell was determined to be 19.4% and the back side was 16,5%, but the double-sensing solar cells with the symmetrical efficiency of 18,4% and 18,1% were also made in the experiment [8]. In this scientific work, a new 3-way sensitive silicon-based solar cell is investigated. Because the 3-way sensitive silicon-based solar cell depicted in Figure 1 is registered as a utility model by the Intellectual Property Agency under the Ministry of Justice of the Republic of Uzbekistan under the number FAP 00623 [9]. But the influence of the environment on its properties has not been studied.

Solar elements are very sensitive to the environment. Therefore, it is important to study the influence of the environment on their properties. For example, the effect of the angle of incidence of light [10] and temperature on the properties of a nanoparticle incorporated solar cell has been studied [11]. Because mainly the solar elements are affected by the temperature and the angle of incidence of light. Therefore, in this scientific work, the effect of temperature on a 3-way sensitive silicon-based solar cell was studied.

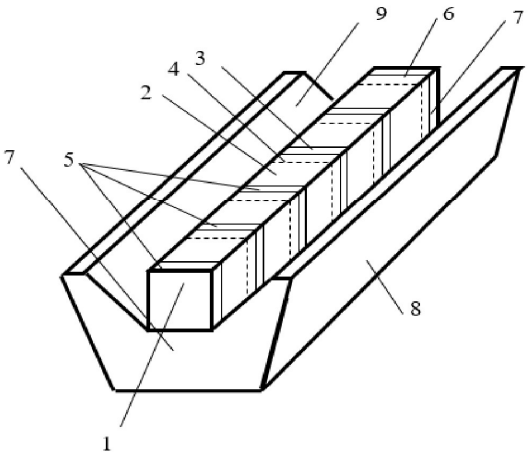

Figure 1. Project of a 3-way sensitive vertical transition solar element
2 – n type, 3 – p type, 4 – p-n junction, 5 – contact layer, 6 – top surface, 7 – side surface, 8 – base

Methods. There are different ways to study physical processes. These are experiment, theory and simulation. In theoretical studies, it is divided into two, obtaining an analytical solution using the fundamental theory of the process and empirical formulas created according to the values determined in the experiment. The simulation method is considered somewhat more complicated. Because, in the process of simulating devices, the fundamental theory and the empirical formula determined in the experiment are used together. The basis of simulation of semiconductor devices is special differential equations. Eigendifferential equations are difficult to calculate using an analytical method,

so numerical methods are used. Because it is possible to algorithmize the calculation sequence through numerical methods and create programs based on this. Primary conditions play an important role in special differential equations. Initial conditions can be in the form of an exact value and a function. Empirical formulas determined in the experiment are mainly used as initial conditions in the modeling of physical processes.

TCAD (Technology Computing Aided Design) programs are widely used in the simulation of semiconductor devices. TCAD is a new family of programs based on CAD programs. CAD programs are mainly designed to create 3D and 2D geometric models of devices. An example of this can be Solidworks or AutoCAD programs. TCAD programs can simulate physical processes in devices by giving them physical properties in addition to creating geometric models of devices. The most common TCAD programs include Sentaurus TCAD, Silvaco TCAD, and Lumerical TCAD. Therefore, the Senaturus TCAD software package from Synopsys was used in this research.

Sentaurus TCAD is a comprehensive software package that includes 23 instruments. It is enough to use 4 instruments to model the solar elements. These are Senataurus Structure Editor, Sentaurus Device, Sentaurus Visual and Sentaurus WorkBench. Each instrument has its own function. In Sentarus Structure Editor, 2D and 3D models of devices are created and meshed for numerical calculations. In Sentaurus Device, physical properties are assigned to the geometric model created in Senaturus Structure Editor, and electrical, optical, and thermal properties of the device are calculated using numerical methods. In Sentaurus Visual, the results obtained on the Sentaurus Device are graphically displayed and visualized. Sentaurus WorkBench serves as a single environment for the above three instruments to exchange information with each other and manage the virtual experience process.

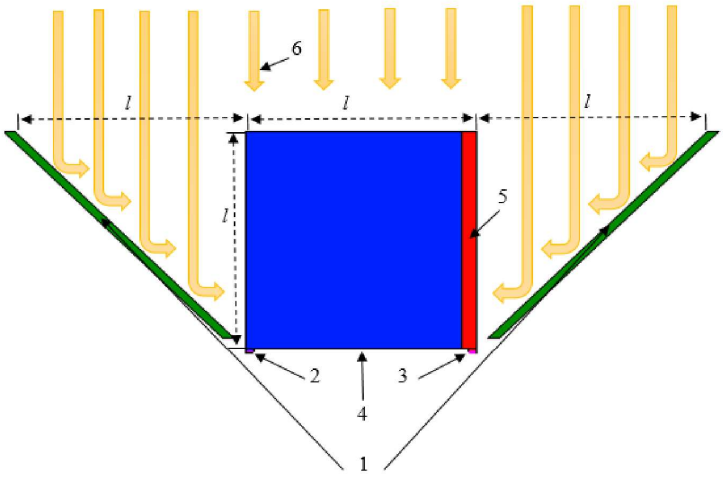

Figure 2. Geometrical model of the solar cell for 3-way lighting and the overall system made in Sentaurus Structure Editor

1 - silver reflectors, 2,3 - contacts, 4 - p type, 5 - n type, 6 - light beam and l - length.

The simplest solar cell consists mainly of front and rear contacts and a p-n junction. To simulate solar elements, their geometric model is developed just like their appearance in real life. Only to speed up the calculation process and increase the calculation accuracy, their size is taken smaller. Figure 2 shows the geometric model of the system developed for three-way illumination of a silicon-based solar cell. In order for light to fall on the three surfaces of the solar cell with the same intensity, the reflective silver is placed at an angle of 45° on both sides. Because the light is emitted parallel to the *p-n* junction.

The light falling on the silver reflectors is directed perpendicularly to the two sides of the solar element. The width and length of the solar element are equal to 175 μm. Boron active atoms in the amount of 10^{15} cm^{-3} are included in the *p* field. Phosphorus active atoms in the amount of 10^{17} cm^{-3} have been included in n field. The thickness of the n field is 3,5 μm and the thickness of the *p* field is 171,5 μm. The AM1,5G spectrum was chosen as the light source.

Theory. The main role in the simulation of semiconductor devices is played by differential equations. For example, to determine the electrical parameters of a simple semiconductor p-n structure in the equilibrium state, it is enough to calculate the Fermi statistics given in formula 1 and the Poisson equation given in formula 2.

$$n = N_c F_{1/2}\left(\frac{E_{F,n} - E_c}{kT}\right) \quad and \quad p = N_V F_{1/2}\left(\frac{E_V - E_{F,p}}{kT}\right) \quad (1)$$

The distribution of the concentration of charge carriers along the semiconductor device is determined with the help of Fermi statistics. It is not possible to calculate the function of Fermi statistics analytically due to the presence of the Fermi half-integral in its composition. The function of Fermi statistics is brought to the Boltzmann approximation by introducing data conditions for calculation in an analytical method. But the Boltzmann distribution gives a more precise value of energy only in a certain range. Since Sentaurus TCAD mainly uses a numerical method, the Fermi function itself was used to calculate the Fermi statistics. Because it is possible to calculate the Fermi function in iterative or numerical methods. The calculated concentration of electrons n and holes p is put into the Poisson equation, and the electric field strength and electric potential distribution in the semiconductor device are determined.

$$\Delta\varphi = -\frac{q}{\varepsilon}\left(p - n + N_D + N_A\right) \quad (2)$$

Modeling solar cells in semiconductor devices is more complicated. Because, in addition to the electrical and thermal properties of solar cells, optical properties should also be taken into account. Sentaurus Device mainly uses Transfer Matrix Method (TMM), Ray Tracing Method and Beam Propagation Method to determine optical properties of solar cells. Each style has its own advantages. For example, the TMM method calculates the optical properties of thin solar cells taking into account the interference phenomenon. The Ray Tracing method was used to determine the optical properties of the system depicted in Figure 2. Because it is necessary to take into account that the light falling on the solar element and silver reflectors will be refracted and populate them. In the Ray Tracing method, a certain number of light rays are sent to the solar cell, and the refracted and reflected parts of each ray are considered as independent rays. When the light intensity is less than the minimum light intensity set during modeling, the calculation of this light is stopped. In turn, the energy of each ray falling on the solar element at the beginning of the simulation is divided into absorbed, released and stopped parts at the end of the simulation. One ray can be divided into more than a thousand rays. A part of these rays can return and pass through the surface of the solar element. This part is considered free rays. It can lose its energy by being absorbed in a solar cell. The remaining part will stop the calculation process before it has enough energy. This part forms the stopped rays. But the total energy of each ray falling on the solar element is equal to the sum of each of them and is calculated based on formula 3.

$$P_{total} = P_{abs} + P_{escape} + P_{stopped} \quad (3)$$

In order to determine the optical properties of the devices, the basic optical parameters such as the refractive index and absorption coefficients of the materials containing the device should be known. In general, the optical parameters of materials are determined by the complex refractive index given in formula 4. The real part of the complex refractive index is the refractive index of the material, and the abstract part is the "excitation coefficient". The light refraction index and "excitation coefficient" of materials depend on the wavelength of light. But the exact function is not defined for each material. Therefore, in the modeling process, the refraction index and the "excitation coefficient" table of dependence on the wavelength of light, created according to the experimental results, are used. This ensures the accuracy and reliability of the optical properties determined by the simulation of the solar cell.

$$n_{tot}(\lambda) = n(\lambda) + ik(\lambda) \quad (4)$$

The absorption coefficient of materials is determined by "excitation coefficient" as given in formula 5.

$$\alpha(\lambda) = \frac{4\pi k}{\lambda} \quad (5)$$

In the Ray Tracing method, certain boundary conditions are included in the calculation of optical properties. Basically, the relationship between the angles of incidence, refraction and return of the light falling on the boundary of two muhts is determined by Snell's law given in formula 6.

$$\frac{n_1}{n_2} = \frac{\sin(\gamma)}{\sin(\theta)}, \quad \beta = \theta \quad (6)$$

The relationship between the energies of the incident, refracted and reflected rays at the boundary of two media is determined by the Fresnel formulas given in formula 7. When Snell's and Fresnel's laws are used as boundary conditions, the coefficients of reflection of light at the boundary of two media change according to the wavelength of light. Because, as mentioned above, the refractive index and absorption coefficient of materials depend on the wavelength of light. Another possibility of Sentaurus Device is to give the transition or return coefficients of two media boundaries as fixed numbers. In this scientific work, Fresnel and Snell's laws were used as boundary conditions in the areas of the solar element in contact with the media. Snell's law and constant reflection coefficient R=1 were used as a boundary condition for the silver reflector (Figure 2.) and the air boundary. The purpose of this is to direct the light falling on the silver reflector perpendicular to the two side surfaces of the solar cell without reducing its energy.

$$\begin{cases} r_t = \dfrac{n_1\cos\beta - n_2\cos\gamma}{n_1\cos\beta + n_2\cos\gamma} \\ t_t = \dfrac{2n_1\cos\beta}{n_1\cos\beta + n_2\cos\gamma} \end{cases} \text{ and } \begin{cases} r_p = \dfrac{n_1\cos\gamma - n_2\cos\beta}{n_1\cos\gamma + n_2\cos\beta} \\ t_p = \dfrac{2n_1\cos\beta}{n_2\cos\beta + n_1\cos\gamma} \end{cases} \quad (7)$$

The amount of electrons and holes formed when light is absorbed in the layers of the solar cell was determined by the optical generation formula given in formula 8. Solar cells have not only optical, but also thermal generation, and this is also taken into account in the modeling of this scientific work. In addition, Auger and Shockley-Read-Hall recombination were also taken into account in the modeling, since the studied solar cell is made of silicon. After that, the total distribution of electrons and holes in the solar cell was calculated using the Fermi function given in formula 1. As written above, the determined concentration of electrons and holes was put into the Poisson equation given in formula 2, and the equation was calculated using a numerical method.

$$G^{opt}(x,y,z,t) = I(x,y,z)\left[1-e^{-\alpha L}\right] \qquad (8)$$

To calculate using the numerical method, the solar cell must be meshed. In this scientific work, the solar element was meshed from 0,01 μm to 0,02 μm on the y axis from a minimum of 0,04 μm to a maximum of 0,08 μm on the x axis. Two types of grids were created to calculate the optical and electrical properties of the solar cell. But the size of their nets was made the same.

$$\nabla \cdot \vec{J}_n = qR_{net,n} + q\frac{\partial n}{\partial t} \quad and \quad -\nabla \vec{J}_p = qR_{net,p} + q\frac{\partial p}{\partial t} \qquad (9)$$

When a photon is absorbed in a solar cell, an electron-hole pair is formed, and due to the internal field created by the p-n junction, they are separated. That is, they will act. When the solar cell is illuminated, charge carriers move and current is generated. The change in the concentration of charge carriers in a specific volume of the solar cell over time creates a current. The relationship between the change in the concentration of electrons and holes over time and the current densities they generate is expressed by the continuity equation given in formula 9. Sentaurus Device has 4 main models for calculating the transfer of charge carriers: Drift-Diffusion, Thermodynamic, Hydrodynamic and Monte Carlo. In Sentaurus Device, the Drift-Diffusion model is the usual model for calculating the migration of charge carriers. That is, if a specific model for calculating the migration of charge carriers is declared in the command file of Sentaurus Device, the program automatically selects the Drift-Diffusion model. In this scientific work, the thermodynamic model given in formula 10 was used to calculate the current density generated by electrons and holes. Because in this model, the effect of temperature on the migration of charge carriers and the phonons generated during the recombination process are also taken into account. However, for this, the temperature equation given in formula 11 should also be calculated. That is, in order to correctly use the Thermodynamic model, it is not enough to declare the Thermodynamic model in the Physics part of the command file of Sentaurus Device, in addition, it is necessary to calculate the Temperature equation in the "Solve" part of the command file. Otherwise, the thermodynamic model gives the same result as the drift-diffusion model.

$$J_n = -nq\mu_n\left(\nabla F_n + P_n\nabla T\right) \quad and \quad J_p = -pq\mu_p\left(\nabla F_p + P_p\nabla T\right) \qquad (10)$$

$$\frac{\partial}{\partial t}\left(c_L T\right) - \nabla\left(k\nabla T\right) = -\nabla\left[\left(P_n T + F_n\right)\vec{J}_n + \left(P_p T + F_p\right)\vec{J}_p\right] - \\ -\frac{1}{q}\left(E_c + \frac{3}{2}kT\right)\left(\nabla\vec{J}_n - qR_{net,n}\right) - \frac{1}{q}\left(E_v + \frac{3}{2}kT\right)\left(-\nabla\vec{J}_p - qR_{net,n}\right) + \hbar\omega G^{opt} \qquad (11)$$

Through the above simulation steps, the effect of temperature on the characteristics of a solar cell with three surfaces was determined.

Results and Discussions. In this scientific work, the photoelectric parameters of a silicon-based solar cell with a width and thickness of 175 μm were determined in 4 different ways, and the effect of temperature on them was studied. Figure 1 shows the volt-ampere characteristics of a silicon-based solar cell with different areas illuminated. The short-circuit current and operating voltage when the light is applied vertically, that is, parallel to the *p-n* junction, were the same as when the light was applied horizontally, i.e., when the light was applied parallel to the p-n junction. The short-circuit current increased by 1,75 times when two-sided illumination compared to one-sided illumination, and 2,81 times when three-sided illumination. The operating voltage of the silicon-based solar cell under double-sided illumination was 2,3% greater than that of single-sided illumination, and 4,7% greater when triple-sided illumination. In the scientific work conducted by Pal, it was determined that the short-circuit current of a silicon-based solar cell with double-sided illumination is 20,1% to 68,1% higher than that of a single-sided one [12].

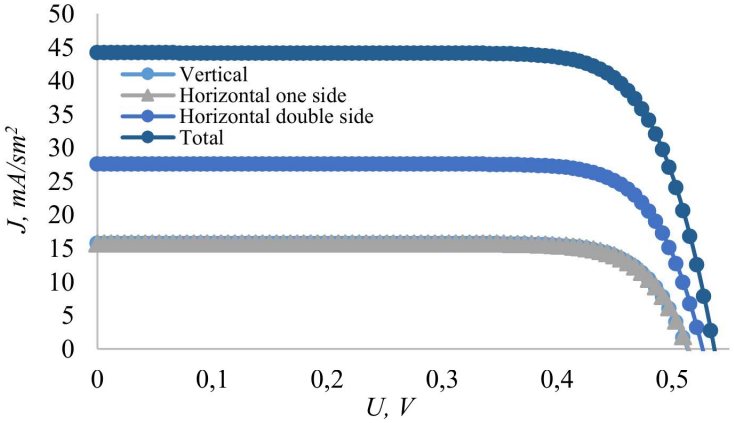

Figure 3. Volt-ampere characteristics of a silicon-based solar cell with different areas illuminated

The main photovoltaic parameters of a solar cell are short-circuit current, operating voltage, fill factor, maximum power and useful duty factor. To calculate these, it is enough to determine the volt-ampere characteristic of the solar cell. Therefore, in this scientific work, the volt-ampere characteristics of the solar cell at different temperatures were calculated and the dependence of the main photoelectric parameters on temperature was determined. The most temperature-sensitive photoelectric parameter is the operating voltage. Therefore, the decrease in the efficiency of the solar cell with the increase in temperature is explained only by the change in the operating voltage. Auger recombination has a greater share in temperature-dependent changes in operating voltage than other recombinations. Figure 4 depicts the temperature dependence of the operating voltage of a silicon-based solar cell with different areas illuminated. The temperature coefficient of the operating voltage for all cases was equal to the same value of $2{,}52\times10^{-3}$ V/K. That is, it turned out that the change of the surface of the solar cell illumination does not have an effect of the operating voltage on the temperature coefficient. In the scientific work of Tiedje, it was determined that the temperature coefficient of the temperature coefficient of the double-illuminated silicon-based solar cell is equal to $1{,}36\times10^{-3}$ V/K [13].

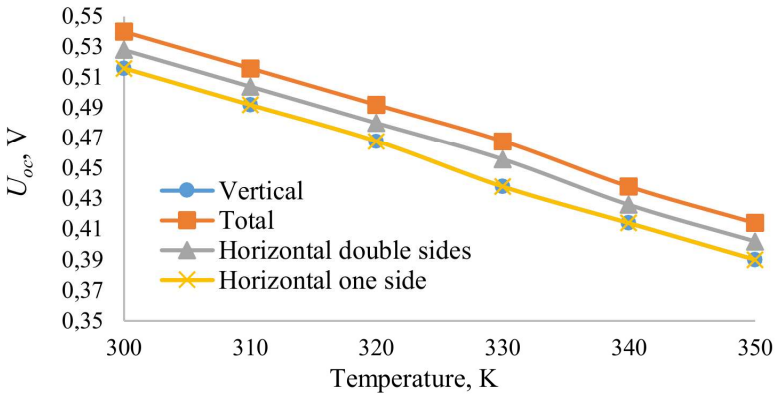

Figure 4. Temperature dependence of the operating voltage of a silicon-based solar cell with different areas illuminated

When the temperature of the solar cell changes, the concentration of phonons inside it and the concentration of electrons and electrons due to thermal generation also changes. Therefore, the short-circuit current should also change due to the dependence on the concentration of charge carriers. Figure 5 depicts the temperature dependence of the short-circuit current of a silicon-based solar cell with different areas illuminated. As shown in Figure 3 above, the short-circuit currents of double- and triple-surface illuminated solar cells are larger than those of single-surface illumination. Therefore, in Figure 4, a graph of the ratio of the short-circuit current at each temperature to the short-circuit current at 300K was created to illustrate the temperature dependence of the short-circuit current. When the temperature changes from 300 K to 350 K, it was found that the short-circuit current decreases by 3,1% when illuminated from one horizontal side, 4,4% when illuminated from two horizontal sides, 3,8% when illuminated from one vertical side, and 4% when illuminated by three surfaces. In an experimental study conducted by He Wang, the short-circuit current temperature coefficient of a silicon-based double-sided sensitive solar module under 600W/m^2 light was determined to be 0,7×10^{-3} K^{-1} [14].

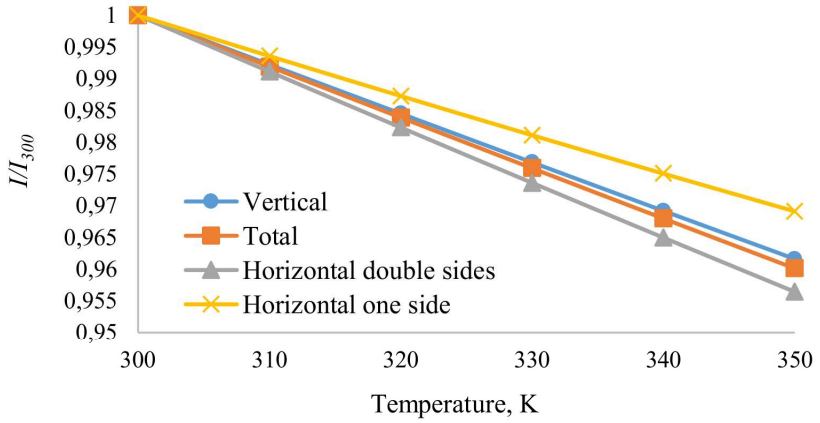

Figure 5. Temperature dependence of the short-circuit current of a silicon-based solar cell with different areas illuminated

The capacity of the solar cells is determined by the fill factor [15]. The value of the fill factor is mainly influenced by the resistance of the solar cell [16][17]. The main role in this is played by the quality of contacts. Figure 6 depicts the temperature dependence of the filling factor of a silicon-based solar cell with different areas illuminated[18][19]. The

fill factor was 2% lower when the total surface was illuminated than when one and both sides were illuminated. An increase in the filling factor was observed for the cases of horizontal and vertical illumination at a temperature of 330K. But for all cases, the function of changing the filling coefficient depending on the temperature has almost the same quality. The temperature coefficient of the filling coefficient was almost the same 1.8×10^{-3} K^{-1} for all cases [20]0. As the temperature increases, the filling coefficient decreases mainly due to the increase in the speed of surface recombination.

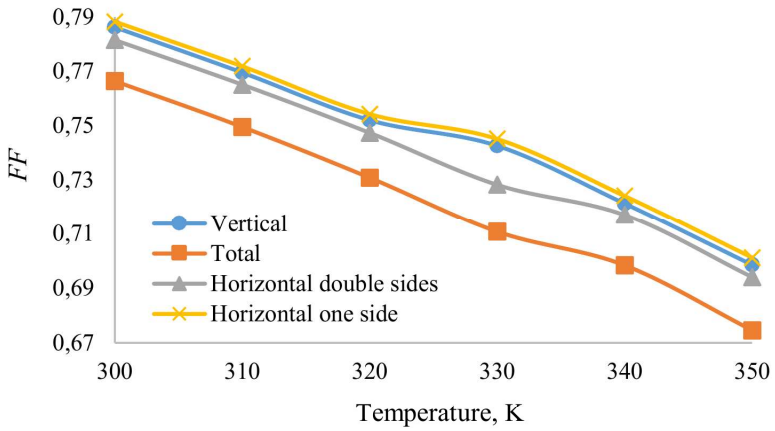

Figure 6. Temperature dependence of the fill factor of a silicon-based solar cell with different areas illuminated

Conclusion. The amount of electricity released from silicon-based solar cells increased with the increase of its illumination surface. Due to this, the concentration of photogenerated electrons and holes in it increases. When the lighting surface increased, it mainly affected the short-circuit current. The operating voltage has not changed much. The efficiency of a silicon-based solar cell decreases with increasing temperature. Also, the efficiency of the solar cell studied in this scientific work has also decreased. When the temperature changes from 300 K to 350 K, it was found that the short-circuit current decreases by 3,1% when illuminated from one horizontal side, 4,4% when illuminated from two horizontal sides, 3,8% when illuminated from one vertical side, and 4% when illuminated by three surfaces. Therefore, the production and use of three-way sensitive solar cells in industry is appropriate.

References

[1]. A. Mardani, A. Jusoh, E. K. Zavadskas, F. Cavallaro, and Z. Khalifah, “Sustainable and Renewable Energy: An Overview of the Application of Multiple Criteria Decision Making Techniques and Approaches,” *Sustainability 2015, Vol. 7, Pages 13947-13984*, vol. 7, no. 10, pp. 13947–13984, Oct. 2015, doi: 10.3390/SU71013947.

[2]. F. M. Guangul and G. T. Chala, “Solar energy as renewable energy source: SWOT analysis,” *2019 4th MEC International Conference on Big Data and Smart City, ICBDSC 2019*, Feb. 2019, doi: 10.1109/ICBDSC.2019.8645580.

[3]. P. Fath, S. Keller, P. Winter, W. Jooß, and W. Herbst, “Status and perspective of crystalline silicon solar cell production,” *Conference Record of the IEEE Photovoltaic Specialists Conference*, pp. 002471–002476, 2009, doi: 10.1109/PVSC.2009.5411274.

[4]. W. Shockley and H. J. Queisser, “Detailed balance limit of efficiency of p-n junction solar cells,” *Journal of applied physics*, vol. 32, no. 3, pp. 510–519, 1961.

[5]. J. Schmidt *et al.*, “Advances in the Surface Passivation of Silicon Solar Cells,” *Energy Procedia*, vol. 15, pp. 30–39, Jan. 2012, doi: 10.1016/J.EGYPRO.2012.02.004.

[6]. R. Aliev, J. Gulomov, M. Abduvohidov, S. Aliev, Z. Ziyoitdinov, and N. Yuldasheva, “Stimulation of Photoactive Absorption of Sunlight in Thin Layers of Silicon Structures by Metal Nanoparticles,” *Applied Solar Energy (English translation of Geliotekhnika)*, vol. 56, no. 5, 2020, doi: 10.3103/S0003701X20050035.

[7]. Mori Hiroshi, “US3278811A - Radiation energy transducing device - Google Patents.” https://patents.google.com/patent/US3278811A/en (accessed Sep. 14, 2021).

[8]. A. Hübner, A. G. Aberle, and R. Hezel, “Novel cost-effective bifacial silicon solar cells with 19.4% front and 18.1% rear efficiency,” *Applied Physics Letters*, vol. 70, no. 8, p. 1008, Aug. 1998, doi: 10.1063/1.118466.

[9]. Aliev Rayimjon, Muxtarov Erkinjon, and Mirzaalimov Avazbek, “Quyosh generator,” FAP 00623, 2011.

[10]. J. Gulomov *et al.*, “Studying the effect of light incidence angle on photoelectric parameters of solar cells by simulation,” *International Journal of Renewable Energy Development*, vol. 10, no. 4, pp. 731–736, 2021, doi: 10.14710/ijred.2021.36277.

[11]. J. Gulomov and R. Aliev, “Study of the Temperature Coefficient of the Main Photoelectric Parameters of Silicon Solar Cells with Various Nanoparticles,” *Journal of Nano- and Electronic Physics*, vol. 13, no. 4, pp. 04033-1-04033–5, 2021, doi: 10.21272/JNEP.13(4).04033.

[12]. S. Pal, A. Reinders, and R. Saive, “Simulation of Bifacial and Monofacial Silicon Solar Cell Short-Circuit Current Density under Measured Spectro-Angular Solar Irradiance,” *IEEE Journal of Photovoltaics*, vol. 10, no. 6, pp. 1803–1815, Nov. 2020, doi: 10.1109/JPHOTOV.2020.3026141.

[13]. T. Tiedje and D. A. Engelbrecht, “Temperature Dependence of the Limiting Efficiency of Bifacial Silicon Solar Cells,” *Conference Record of the IEEE Photovoltaic Specialists Conference*, vol. 2020-June, pp. 1789–1791, Jun. 2020, doi: 10.1109/PVSC45281.2020.9300921.

[14]. H. Wang, X. Cheng, and H. Yang, “Temperature Coefficients and Operating Temperature Verification for Passivated Emitter and Rear Cell Bifacial Silicon Solar Module,” *IEEE Journal of Photovoltaics*, vol. 10, no. 3, pp. 729–739, May 2020, doi: 10.1109/JPHOTOV.2020.2974289.

[15]. J. Zhou, Q. Huang, Y. Ding, G. Hou, Y. Zhao, Nano Energy 92, 106712 (2022).

[16]. Solar PV – Analysis – IEA. (2023).

[17]. B. Grübel, G. Cimiotti, C. Schmiga, S. Schellinger, B. Steinhauser, A. A. Brand, M. Kamp, M. Sieber, D. Brunner, S. Fox, S. Kluska, Prog. Photovolt.: Res. Appl. 30 No 6, 615 (2022).

[18]. Z. Sun, X. Chen, Y. He, J. Li, J. Wang, H. Yan, Y. Zhang, Adv. Energy Mater. 12 No 23, 2200015 (2022).

[19]. J. Gulomov, R. Aliev, J. Nano- Electron. Phys. 13 No 6, 06036 (2021).

[20]. Y. Da, Y. Xuan, Q. Li, Sol. Energy Mater. Sol. C. 174, 206 (2018).

M. Abderrezek, M. Fathi, F. Djahli, J. Nano- Electron. Phys. 10, No 2, 02027 (2018).

CONTENTS